

Research Paper

Study on the Impact of Drainage Noise in Residential Bathrooms Based on Finite Element Simulation

Yaping WANG, Xin DENG, Bingyuan CHI, Yanqiu CUI*

*School of Architecture and Urban Planning, Shandong Jianzhu University
China**Corresponding Author e-mail: cyq@sdjzu.edu.cn*(received June 8, 2023; accepted March 28, 2024; published online June 18, 2024)*

Residential bathroom drainage noise is a primary source of indoor noise that directly affects quality of life and physical and mental health. Therefore, based on the acoustic theory and the finite element simulation technology, this paper proposes a method to simulate the drainage noise characteristics and its impact range jointly using the flow and acoustic fields. The pressure at the pipe wall caused by the internal flow field of the bathroom drainage pipe is calculated by the Fluent software. Simulations are carried out with the Virtual Lab software to predict the drainage noise characteristics and spatial distribution and to analyse the influence of factors such as the door position, riser position, and the partition wall material on the noise distribution. The results show that drainage noise has prominent high-frequency characteristics, the position of the bathroom drainage pipes and doors affects the spatial noise distribution, and the sound insulation performance of a partition wall with ordinary fired bricks in the bathroom is slightly better than that of ordinary concrete bricks, lightweight aggregate concrete blocks or fly ash blocks. This paper provides a theoretical basis and practical reference for reducing the impact of residential drainage noise and creating a healthy and comfortable indoor acoustic environment.

Keywords: residential building; bathroom drainage noise; numerical simulation; sound field distribution.



Copyright © The Author(s).
This work is licensed under the Creative Commons Attribution 4.0 International CC BY 4.0
(<https://creativecommons.org/licenses/by/4.0/>).

1. Introduction

With the rapid development of society, public demand for environmental quality has gradually increased. Noise is one of four major environmental pollutants in the world and has become a key concern. Residential spaces are most closely associated with people's daily lives, and indoor noise can significantly reduce quality of life, work efficiency and health; notably, residential bathroom drainage noise is a primary source of indoor noise (PARK *et al.*, 2018; PUJOL *et al.*, 2014). Previous studies have used field tests, laboratory tests, numerical simulations, subjective evaluations, and virtual reality to explore the objective parameters of residential bathroom drainage noise and residents' subjective evaluations and have found that drainage noise causes significant disturbance to residents (JEON *et al.*, 2019; RYU, SONG, 2019). Therefore, research on residential bathroom drainage noise characteristics and radiated sound fields is essential for cre-

ating a healthy and comfortable acoustic environment in living spaces.

Pipe drainage noise research worldwide has focused mainly on the causes of noise and the factors influencing it, as well as noise reduction control measures, and the prediction, numerical simulation of flow noise, and radiation sound fields.

One study reported that the causes of pipe drainage noise include water flow impact, air pressure fluctuations, and water flow direction mutation. The leading cause was determined to be unstable water and air pressure in a non-full flow pipe (FUCHS, 1983; 1993a). Additionally, factors such as the drainage method, pipe material and fittings, sanitary ware, water flow velocity, and pressure can significantly affect drainage noise (FUCHS, 1993b; VILLOT, 2000). Laboratory tests of UPVC pipe drainage noise revealed that the noise impact of the same-floor drainage pipes was lower than that of different-floor drainage pipes (YANG *et al.*, 2016). Increasing the wall thickness of new UPVC

pipes or increasing the material density of pipes could reduce the impact of drainage noise (JEONG *et al.*, 2017; YEON *et al.*, 2014), and the drainage noise of a vacuum double-bend pipe was approximately 3.5 dB(A) lower than that of an ordinary pipe (JUNG *et al.*, 2012). In addition, the use of new low-noise systems and connections (JEONG *et al.*, 2017; YEON *et al.*, 2014), the use of pipe cladding, the addition of pipe wells, and other measures (XU *et al.*, 2014) were also found to reduce noise.

In recent years, numerical simulation methods, mainly including the sound line method, the finite element method, the boundary element method, and the statistical energy method, have gradually become important research tools in architectural acoustics. Among them, the finite element and boundary element methods are simulation methods based on the wave acoustic theory (MARBURG, NOLTE, 2008) and are widely used in research on pipe noise and enclosed sound fields.

Previous studies have used finite element methods to analyse the coupled vibration noise of pipes and simulate the external radiated sound field of pipes (LIANG *et al.*, 2006; MORI *et al.*, 2017). The vibration noise of gas transmission pipe systems is simulated via ANSYS and SysNoise (LIU *et al.*, 2016; HAN *et al.*, 2020). The acoustic, vibration, and aeroacoustic noise characteristics of *T*-shaped and rectangular cross-section tubes were simulated by experiments with different flow velocities and finite element simulations (MORI *et al.*, 2017). The Virtual Lab software was used to investigate the flow noise propagation mechanism in pipes based on the flow and sound field synergy principle (CAO *et al.*, 2017). CFD was used to analyse the characteristics and main factors influencing flow-induced noise in the variable cross-section pipe. The flow-induced noise and flow field characteristics, including the sound source intensity distribution, pressure distribution, velocity distribution, and spectrum of sound pressure level, were obtained. This provided a theoretical basis for the optimization of variable cross-section piping systems and the investigation of flow-induced noise control techniques (SUN *et al.*, 2021). Additionally, in the context of enclosed space sound fields, the COMSOL Multiphysics software has also been used to evaluate the effect of the addition of sound absorption and the change in absorption position on the sound field in small rooms. This method allows more accurate calculation of low-frequency sound field data in rooms (LAU, POWELL, 2018).

In summary, previous studies have explored the generation principles, characteristics, and factors influencing residential bathroom drainage noise. The flow-induced noise of pipes has a significant impact on the indoor acoustic environment of adjacent floors, and the use of silent pipes, wrapping acoustic insulation materials, and other measures have been proposed to

reduce drainage noise. These works provide an essential theoretical and practical basis for future research. However, in previous studies of pipe drainage noise, most of the flow noise in the pipe was assumed to arise from a line sound source, supplemented by a constant flow rate and flow velocity to the actual noise measurement, which cannot sufficiently reflect the actual state of fluid flow in the pipe, and there is a certain discrepancy with the actual sound field.

In recent years, the use of finite element and boundary element methods with simulation software such as Ansys and COMSOL to simulate fluid flow within pipes and enclosed space sound fields has become a target of active research. However, there has been a relative lack of research on predicting bathroom drainage noise and its radiation distribution using numerical simulation methods. Therefore, this paper proposes a method for predicting pipe drainage noise and its effects using finite element simulation techniques with the help of the numerical simulation software Ansys Fluent (version 2020) and LMS Virtual Lab (v13.6), analyses the factors affecting the noise sound field, and proposes noise reduction design recommendations, providing new ideas and methods for indoor sound environment research.

2. Numerical simulation methods

Pipe drainage noise, which is generated by the interaction between the fluid inside the pipe and the pipe wall, includes the flow noise generated by fluid motion inside the pipe and the radiation noise generated by the vibration of the pipe wall. Therefore, based on a theory related to flow and vibration noise, a method of simulating the indoor drainage noise distribution using joint simulation of the flow field and sound fields is proposed, as shown in Fig. 1.

2.1. Theoretical analysis of pipe drainage noise

2.1.1. Flow noise

The root cause of flow noise is that the fluid flow produces a distributed sound source throughout the flow field, which is considered aeroacoustics and is generated by the interaction of the fluid medium, the solid wall, and the sound field (LIGHTHILL, 1952; CURLE, 1955; FLOWCS WILLIAMS, HAWKINGS, 1969). The effect of a solid wall on flow-induced noise is considered, and the FW-H equation elucidates three types of flow noise sources in terms of the occurrence mechanism, namely, monopole sources generated by fluid volume pulsations, dipole sources generated by pulsations at solid boundaries, and quadrupole sources generated by free fluid turbulence (LIGHTHILL, 1952; CURLE, 1955; FLOWCS WILLIAMS, HAWKINGS, 1969; ZHANG *et al.*, 2016). The flow in the drainage pipe of

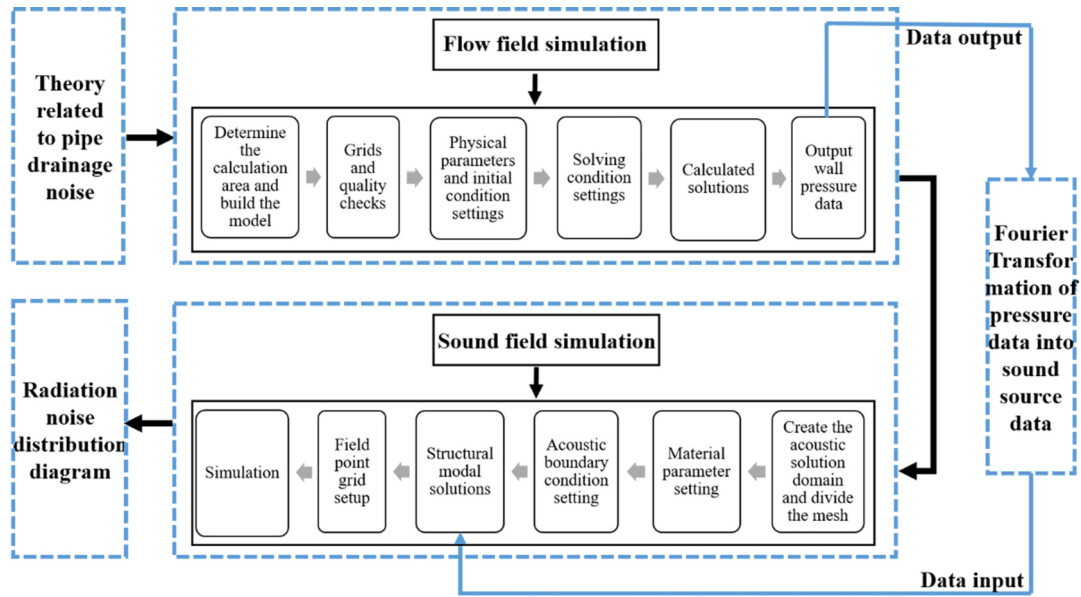


Fig. 1. Numerical simulation process for the radiated sound field of pipe drainage noise.

the residential bathroom is a type of gas-liquid two-phase flow with the low Mach number; the flow velocity is much lower than the sound velocity, the boundary condition is a static solid wall, the compressibility effect of the mixed fluid is negligible, and the fluid acceleration is weak. Therefore, the effect of monopole sources and quadrupole sources on the noise can be ignored, and the noise sources in the flow field are treated as distributed dipole sources caused by pressure pulsations generated by the flow field near the wall surface.

2.1.2. Vibration radiation noise

The mixed fluid in the drainage pipe impacts the wall to excite structural vibration, generating structural noise and propagating to the space inside and outside the pipe, producing indoor interference noise. From the perspective of the vibration generation mechanism, the vibration of thin-walled pipes derives from the excitation and transmission of fluid motion, which is influenced to some extent by characteristics such as the intensity of turbulent motion. The vibration is also influenced by the physical properties of the structure itself, with the frequency characteristics of some structural components (NORTON, KARCZUB, 2003a; NORTON, BULL, 1984).

The inherent properties of structural vibrations are described by structural modes, which are related only to the shape and dimensions of the structure and the external excitation frequency (NORTON, KARCZUB, 2003b; MAO, PIETRZKO, 2013). Analysis of the structural modes can reveal the vibration characteristics of a structure, predicting its vibration response under external excitation conditions and hence the distribution of radiated noise.

2.2. Simulation method and process

2.2.1. Flow field simulation method and process

This paper uses the CFD software Fluent, which is integrated with the Ansys Workbench environment, to simulate the internal flow field characteristics of a bathroom drainage pipe, to obtain the flow state of the mixed media inside the drainage pipe, and to output the pressure data on the inner wall of the pipe as the sound source parameters for acoustic analysis. The calculation models include the VOF multiphase flow model and the realizable $k-\varepsilon$ turbulence model. The primary process of using the Fluent software to simulate and analyse the flow field information in the pipe is shown in Fig. 1.

2.2.2. Sound field simulation method and process

The paper utilizes the Virtual Lab software to simulate the sound field distribution in the interior space using the model-based finite element method. The sound field simulation process is shown in Fig. 1. Firstly, the acoustical solution domains for the inside of the pipe and the room are created in the Virtual Lab software, and the automatic matching layer (AML) is used. Then, the three-dimensional body mesh of the solid air domain is generated. The division of the acoustic mesh should meet the requirement that the minimum unit size is no greater than one-sixth of the wavelength corresponding to the maximum frequency, as shown in Eq. (1):

$$L_s \leq \frac{c_{\text{air}}}{6f_{\text{max}}} \quad (1)$$

The material parameters are set for the acoustical computational domain and the exterior-protection

construction. The wall pressure data obtained from the flow field simulation are used as the excitation conditions for the sound field. The structural modes required for acoustic simulations are calculated based on the Nastran platform. Finally, the field point grid is set up to monitor the simulation results.

2.3. Simulation of model settings

2.3.1. Plan forms

The bedroom adjacent to the bathroom in the residence is the area most severely disturbed by drainage noise. Therefore, this paper takes the master bedroom suite with a bathroom as the base model to study the sound field distribution of drainage noise in the bedroom. The base model plane of the master bedroom suite and its dimensions are determined according to the Chinese standard GB 11977-2008 (Standardization Administration of the P.R.C., 2008), as shown in Fig. 2.

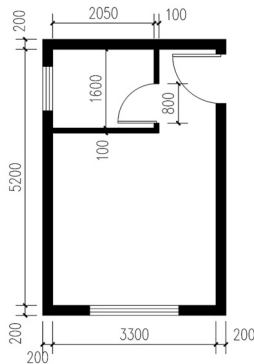


Fig. 2. Basic model plan.

This study focuses on the propagation of pipe drainage noise in a bedroom space. To simplify the model and facilitate calculations, only factors such as the position of the bathroom door, the position of the riser, and the material of the partition wall are considered. The lateral sound transmission effects of the external walls, floor, and other components are disregarded. The positions of the bathroom doors are shown in Fig. 3, and the positions of the riser arrangements are shown in Fig. 3c. To study the most unfavourable

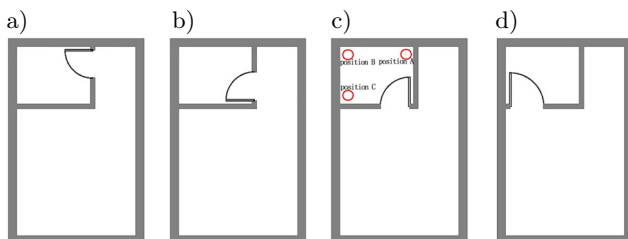


Fig. 3. Schematic diagram of the bathroom and plumbing positions: a) position 1; b) position 2; c) position 3; d) position 4.

case of noise impact, the bathroom door is set to be open. The partition wall between the bathroom and the bedroom is a block infill wall, and the material and thickness of the partition wall are shown in Table 1.

Table 1. Material and wall thickness of the bathroom partition walls.

Masonry materials	Ordinary fired brick	Ordinary concrete bricks	Lightweight aggregate concrete block	Fly ash block
Masonry thickness [mm]	120	100	100	100

2.3.2. Drainage methods

The common drainage methods used in residential bathrooms are the same-floor and different-floor drainage. At present, the most widely used method of drainage in China's completed ordinary houses is different-floor drainage. However, during the drainage of upper-floor occupants, the flow noise and wall vibration noise from flow impacting the pipe section can have a serious impact on the lower floors (YANG *et al.*, 2016). In addition, the toilet is the sanitary ware with the highest incremental sound pressure level of drainage noise (JEONG *et al.*, 2017), so this paper uses a toilet drainage system with different-floor drainage as the simulation model.

2.3.3. Pipe forms

Currently, depending on the combination of drainage and ventilation pipes, common UPVC single-riser and double-riser systems are more widely used in residential bathrooms in China. Compared with single risers, double risers are equipped with ventilation piping, which balances the air pressure and reduces the noise of air plugs. Therefore, the noisier single riser system is chosen as the base model (JIANG, WU, 2019). The pipe material is UPVC. The pipe size was determined according to the Chinese standard GB 50015-2019 (Ministry of Housing and Urban-Rural Development, China, 2019), as shown in Table 2.

Table 2. Drainage pipe simulation model sizes.

Parameter	Symbol	Value
Pipe diameter [mm]	D	110
Pipe wall thickness [mm]	–	3.2
Height of riser [mm]	H_1	2700
Length of transverse branch pipe [mm]	L_1	550
Slope of transverse branch pipe [°]	–	1.49
Height of sanitary ware pipe [mm]	H_2	200
Length of sanitary ware pipe [mm]	L_2	150

3. Drainage pipe sound source simulation

3.1. Wall pressure due to the flow field in the drain

3.1.1. Simulation model building

According to the pipe form model setting in Subsec. 2.3.3, the fluid simulation model of the internal flow field of the single riser system is created in the CATIA platform, as shown in Fig. 4.

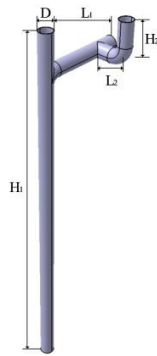


Fig. 4. Fluid simulation model.

The overall model is divided with a tetrahedral mesh, with boundary layers added near the walls. In addition, local mesh encryption is carried out at the intersection of the riser pipe and the transverse branch pipe, the transverse branch pipe and the sanitary ware drainage pipe, as shown in Fig. 5.

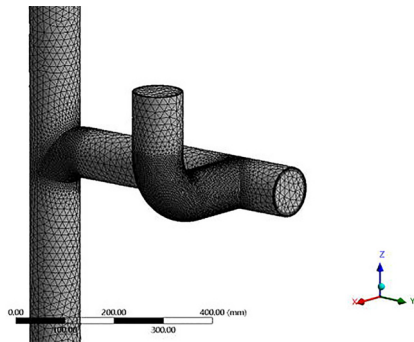


Fig. 5. Illustration of local grid encryption.

Finally, the number of mesh elements in the fluid computational domain reaches 3.5 million, the maximum value of the mesh skewness is $0.76 < 0.9$, and the minimum value of the orthogonal quality parameter is $0.32 > 0.2$. The overall mesh quality meets the Fluent solution requirements.

3.1.2. Simulation parameter settings

3.1.2.1. Boundary condition setting. The boundary conditions are set consistent with the actual drainage process. The inlet of the sanitary ware pipe is defined as the velocity inlet, and the siphon toilet, which is widely used in China, was selected as the upper floor drainage appliance, with the inlet flow velocity set at

$v = 1.0$ m/s. Moreover, the total flow rate of the primary drainage is controlled by writing the equation of the velocity at the inlet and the proportion of each phase, adjusting the velocity inlet to stop feeding water when the total flow reaches the primary drainage of the toilet, that is, $4.8 L$. The velocity at the inlet is automatically adjusted to $v = 0$ m/s. The other inlets of the pipe are pressure inlets, and the inlet pressure is $p = 0$ Pa. The bottom cross-trunk pipe outlet is set as a pressure outlet with a pressure value of 0 Pa. The diameter of each pipe section is 103.6 mm, and the turbulence intensity is 5% . The pipe wall is set as a no-slip interface, and the wall roughness is set according to the wall material. The roughness is 0.009 mm when the wall is made of plastic, such as UPVC.

3.1.2.2. Solution setup. A double-precision solver was selected for this simulation. The pressure-velocity coupling is based on the pressure-implicit with splitting of the operator (PISO) algorithm. The discrete pressure format is set to body-force-weighted. The pressure and momentum terms are both second-order upwind terms, and the gradient is based on the least squares cell. The number of time steps is set to 3.2×10^4 .

The flow field within the height range of the sound field simulation is selected, and the wall pressure data obtained are used as the acoustic boundary conditions for the subsequent simulation. In addition, the time step size of the transient simulation directly affects the frequency range of the acoustic simulation, and the quantitative relationship between the two is shown in Eq. (2):

$$t_s = \frac{1/f_{\max}}{2}. \quad (2)$$

In the sound field simulation, the highest frequency of interest in this study is 4000 Hz, and the time step size of the flow field simulation is set to 1.25×10^{-4} s based on the relationship between the step size and frequency.

3.1.3. Field-induced wall pressure data

The vibration noise generation principle is described in Subsec. 2.1.2. For the bathroom pipe drainage process, the water flows to a certain flow rate from the upper end of the sanitary ware drainage pipe under the joint action of gravity and wall friction along the ware drainage pipe into the drainage transverse branch pipe and drainage riser, and the wall of the pipe at each connection produces constant changes in the impact, inducing vibration of thin-walled pipes and driving fluctuations in the external air medium, causing fluctuations in the sound pressure in the space and thus spreading the drainage noise to the indoor space. Therefore, the analysis of the pressure distribution on the wall surface of the pipe is the analysis of the sound source of pipe vibration.

Fluent transient calculations are used to simulate the primary drainage process of the toilet, intercepting part of the flow field in the room and calculating the pipe wall pressure at each time step in that range. As the pipe drainage is constantly changing, the velocity and pressure field distributions in the computational domain vary at each moment. When analysing the change in pressure distribution at the pipe wall during the primary drainage process, as the fluid flows through each section of the pipe, the pressure distribution at each part of the pipe wall within the height range of the interior space shows a specific change rule. To demonstrate the everchanging pipe wall pressure distribution, at 0 s–2 s, representative time points in different periods of fluid motion changes are selected to indicate the distribution of the pipe wall pressure in that period, as shown in Fig. 6.

Fluid starts to flow into the pipe from $t = 0$ s. During the period from 0 s to 0.2 s, as shown in Fig. 6a, the pressure is positive in all areas except for the inlet pipe section, which is negative, and the pressure increases as the drainage volume increases. During the period from 0.2 s to 0.38 s, the fluid flows through the bend of the drainage apparatus pipe, and the vertically falling fluid has a significant impact on the outer wall of the bend, as shown in Fig. 6c, where the pressure gradually increases and is much greater than the wall pressure at other locations. From 0.38 s to 0.85 s, the fluid moves from the sanitary ware drain pipe to the drain transverse branch pipe, the impact of the fluid on the outside of the bend gradually decreases, the range of the negative pressure zone extends to the upper sidewall of the transverse sanitary ware drain pipe, as shown in Fig. 6c, and the maximum positive pressure value is reached at $t = 0.422$ s. During the 0.85 s to 1.15 s period, the fluid moves mainly in the drain transverse branch pipe, and the extent of the negative pressure zone at the inlet increases further, while its pressure decreases. After this period, the fluid in the transverse branch pipe starts to move into the riser, the outer wall at the intersection of the riser and transverse branch

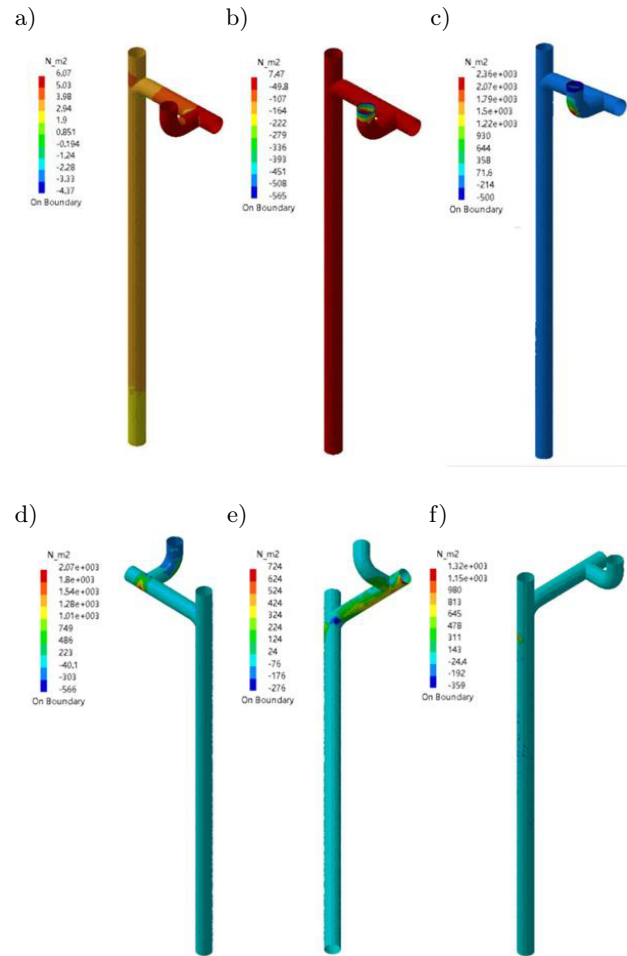


Fig. 6. Pressure distribution at the pipe wall at different moments: a) $t = 0$ s; b) $t = 0.2$ s; c) $t = 0.256$ s; d) $t = 0.422$ s; e) $t = 1.142$ s; f) $t = 1.782$ s.

pipe is subjected to a greater impact of the fluid, and a positive pressure zone starts to appear, but the area and pressure values of the positive pressure zone are smaller than before, as shown in Fig. 6f.

The maximum pressure data and the location of the wall surface at different times of the drainage process are shown in Table 3. A maximum negative pressure

Table 3. Maximum wall pressure data and locations at different times.

Period [s]	Maximum positive pressure value [N/m ²]	Maximum positive pressure position	Maximum negative pressure value [N/m ²]	Maximum negative pressure position
$t = 0-0.2$	<10	Other areas outside the inlet pipe section	More than -560	Inlet pipe section
$t = 0.2-0.38$	4.32×10^3	At the bend	Above -500	Inlet to the area above the bend
$t = 0.38-0.85$	2.07×10^3	A lower sidewall of the bend at the junction with the transverse branch pipe	Approximately -300	An upper sidewall of the bend where it meets the transverse branch pipe
$t = 0.85-1.15$	0–800	A lower sidewall of the transverse branch pipe	–	Upper sidewalls of sanitary ware drains and drainage of the transverse branch pipe
$t = 1.15$ later	1.32×10^3	Outer pipe wall at the junction of the riser and the transverse branch pipe	–	–

of more than -560 N/m^2 occurs during the 0 s to 0.2 s period, and a maximum positive pressure of $4.32 \times 10^3 \text{ N/m}^2$ occurs during the 0.2 s to 0.38 s period.

The impact of the water flow on the wall at different locations in the drainage process is constantly changing with the fluid movement, and the vibration of the pipe wall generated by the impact also changes at all times, with a larger pipe wall impact in the 0 s–1 s period. Therefore, the pressure data in the 0 s–1 s period are selected as the sound source for the acoustic simulation to simulate the impact of vibration noise caused by the fluid impacting the pipe wall at different locations within the pipe.

3.2. Pipe sound field simulation

3.2.1. Simulation model and parameters

In practice, the flow field and the solid wall are coupled, and the change in the fluid flow characteristics inside the pipe has a large impact on the solid wall of the pipe. Therefore, the vibration modal and acoustic finite element methods are used to analyse the acoustic characteristics of noise in the pipe under fluid–solid coupling using the LMS Virtual Lab software. A three-dimensional geometric model of the pipe wall and the sound field inside the pipe was created based on the pipe dimensions described in Subsec. 2.3.3. A tetrahedral mesh of the structural and acoustical computational domains is delineated and extracted. The upper-frequency limit of interest for this simulation is 4000 Hz, and the mesh size of the pipe wall and the internal acoustic field is 14 mm, as shown in Fig. 7.

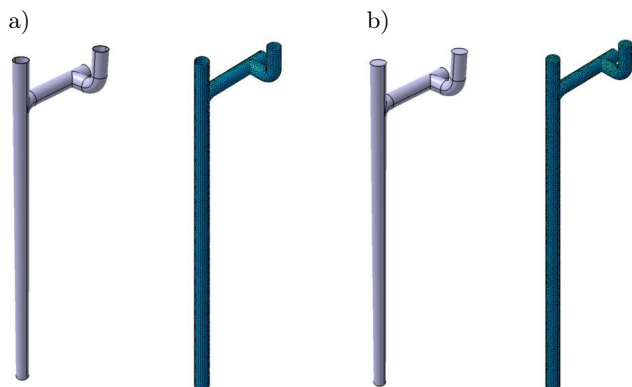


Fig. 7. Geometric modelling and meshing: a) pipe wall models and structural meshes; b) fluid domain and acoustic mesh in pipe.

The structural grid of the pipe wall is made of UPVC material. The material has Young’s modulus of 3.14×10^9 , Poisson’s ratio of 0.32, and a density of 1400 kg/m^3 . The volume proportion of water inside the pipe is so small that its effect is negligible. The material of the fluid domain in the pipe is set to air. The

wall pressure data in the 0 s–1 s time interval are used as the source conditions for the acoustic simulation, and the acoustic–vibrational coupling method is used in the acoustic finite element analysis module to simulate the distribution of the sound field inside the pipe.

3.2.2. Pipe wall vibration modes

The vibration modes of the pipe wall are calculated in the noise and vibration module. Constraints are set in the middle of the riser and the transverse branch pipe to simulate the fixing effect of the pipe clamps and displacement constraints are set in the x -, y -, and z -directions at the upper and lower cross-sections of the riser and the upper cross-section of the sanitary ware pipe. Since the frequency range of concern for acoustic simulation is 100 Hz–4000 Hz, the modal solution range is set slightly larger than the acoustic solution range, which is 90 Hz–4010 Hz. The vibration modes of several frequencies are intercepted, as shown in Fig. 8.

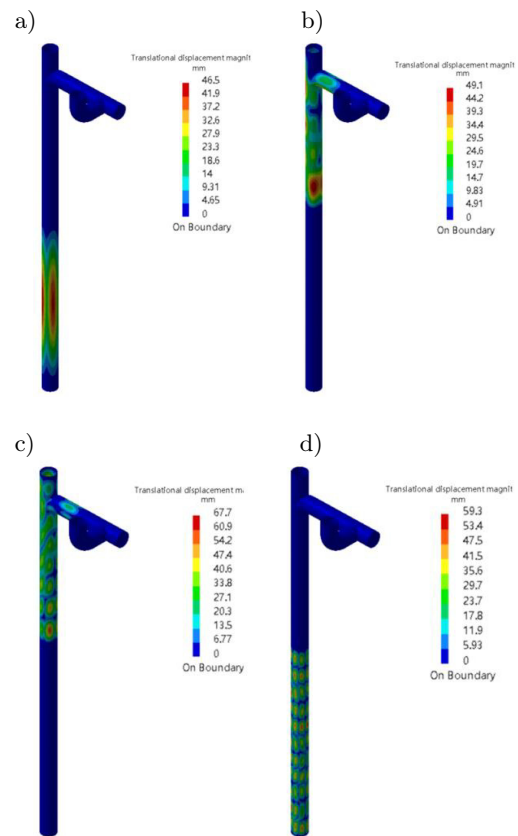


Fig. 8. UPVC pipe vibration modes: a) 250 Hz; b) 500 Hz; c) 1000 Hz; d) 2000 Hz.

The simulation results show that with the gradual increase in frequency, the vibration amplitude of the pipe wall gradually increases, and the maximum value of its vibration displacement gradually increases from 39.1 mm near 125 Hz to 129 mm near 4000 Hz. Due to the constraint effect of pipe clamps, the deformation

degree of different positions of the pipe is very different at the same frequency. For example, in Fig. 8b, the vibration deformation of the pipe at 500 Hz is mainly concentrated in the upper part of the riser, and the maximum vibration displacement in the middle can reach 49.1 mm, while the vibration deformation of the lower part of the riser and the transverse branch is smaller, and the resulting displacement can be ignored.

3.2.3. Sound field distribution inside the pipe

Based on the structural modal simulation results, the sound field distribution inside the pipe under external motivation is calculated. Sound pressure level monitoring points are set up in the acoustic solution domain at the positions shown in Fig. 9 to observe the radiated noise at different positions inside the pipe. A cloud diagram of the sound pressure level distribution in the solution domain is shown in Fig. 10a.

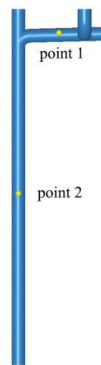


Fig. 9. Distribution of measurement points.

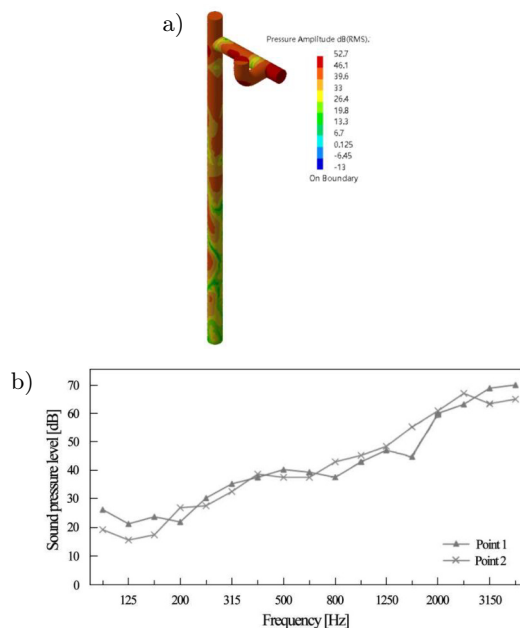


Fig. 10. Sound pressure level distribution cloud and spectral distribution of the measurement points: a) sound field distribution inside the pipe (1000 Hz); b) spectrum of sound pressure levels at monitoring points.

The spectral distribution of each observation point is shown in Fig. 10b.

The results show that the rheological vibration noise inside the pipe exhibits notable high-frequency characteristics, and the sound pressure gradually increases with increasing frequency. The maximum value occurs in the high-frequency range of 2000 Hz–4000 Hz, and the maximum sound pressure can reach more than 70 dB.

4. Results of the radiation sound field distribution of pipe drainage

To investigate the effects of the door position, pipe position, and partition wall material on the distribution characteristics of pipe drainage noise in the bathroom and the adjacent usable space.

4.1. Simulation model setup

4.1.1. Model building

According to the model settings in Subsec. 2.3, structural components such as pipe walls and bathroom partition walls are established in LMS Virtual Lab, and the three-dimensional geometric model of the interior acoustic solution domain is shown in Fig. 11. The positions of the different doors and pipes in the bathroom are shown in Table 4.

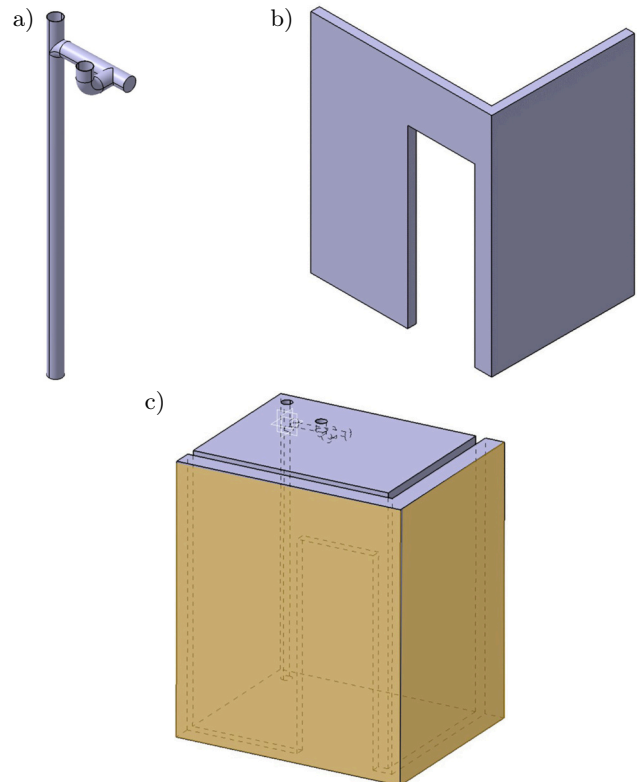
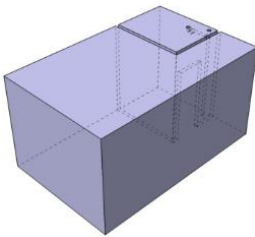
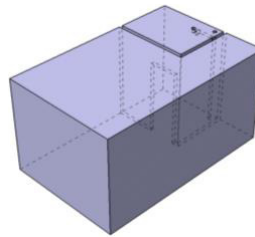
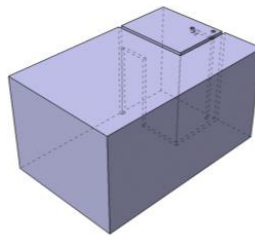
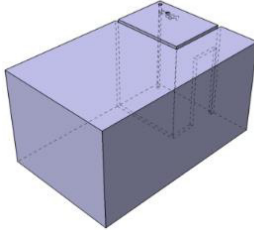
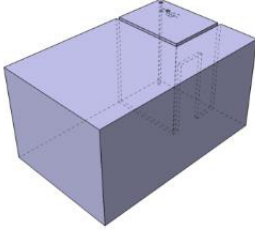
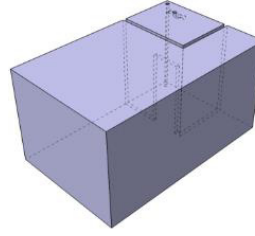
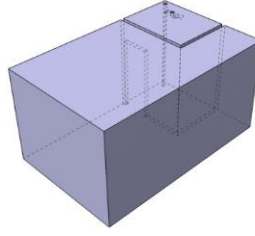
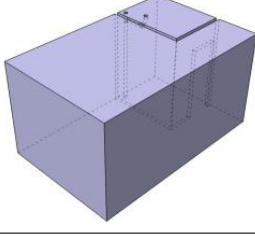
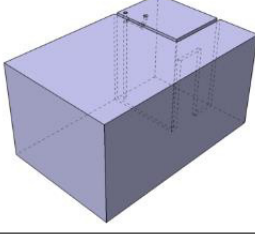
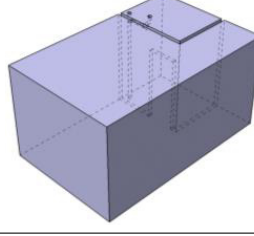


Fig. 11. Simplified simulation model of the residential bathroom: a) pipe wall; b) bathroom partition wall; c) AML boundary layer.

Table 4. Acoustic model settings.

Pipe positions	Door positions			
	1	2	3	4
A	(positions overlap)			
B				
C			(positions overlap)	

A, B, and C represent different pipe positions, with 1, 2, 3, and 4 representing different door positions in the bathroom, excluding the A1 and C3 working conditions where the pipe and door positions overlap, forming a total of 10 different working conditions.

4.1.2. Parameter setting

The mesh size of the pipe wall structure and the bathroom partition wall is set to 20 mm, and the mesh size of the indoor acoustic domain is set to 14 mm considering the upper limit of the simulation frequency and the computer performance. A field point grid and noise monitoring points were set up 1.2 m above the indoor floor to observe the distribution of drainage noise in the interior space. The structural mesh is imported into the noise and vibration module, and the contact surface between the partition wall and other surrounding enclosure components is set as a fixed constraint to determine the structural mode of the partition wall in the acoustic calculation frequency range.

4.2. Analysis of the sound field simulation results

4.2.1. Influence of the door position

To analyse the influence of the door position on the noise distribution of the pipe drainage in the external space, the partition wall material is set as ordinary concrete brick, and the pipe position in the model B is

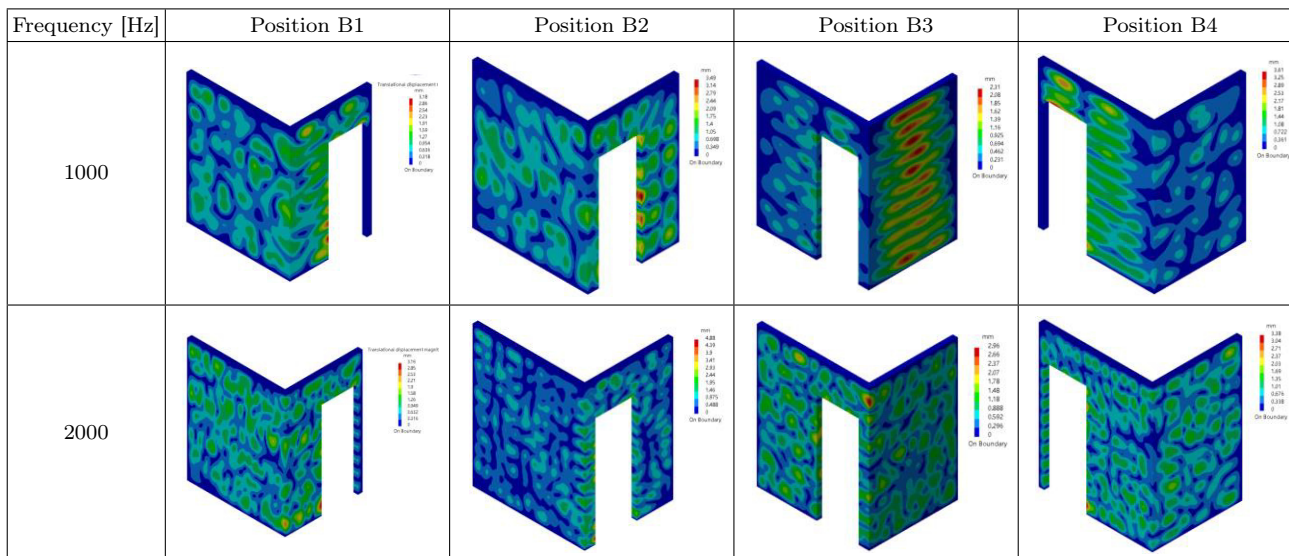
used. For different door positions, the drainage noise distribution is calculated under working conditions B1, B2, B3, and B4. The structural modes of the partition wall caused by pipe drainage in the acoustic calculation frequency range for medium frequencies of 1000 Hz and 2000 Hz are shown in Table 5.

The spatial sound field distribution at different door positions in the bathroom is simulated, and the results are shown in Fig. 12. The noise spectrum at the indoor monitoring points is shown in Fig. 13.

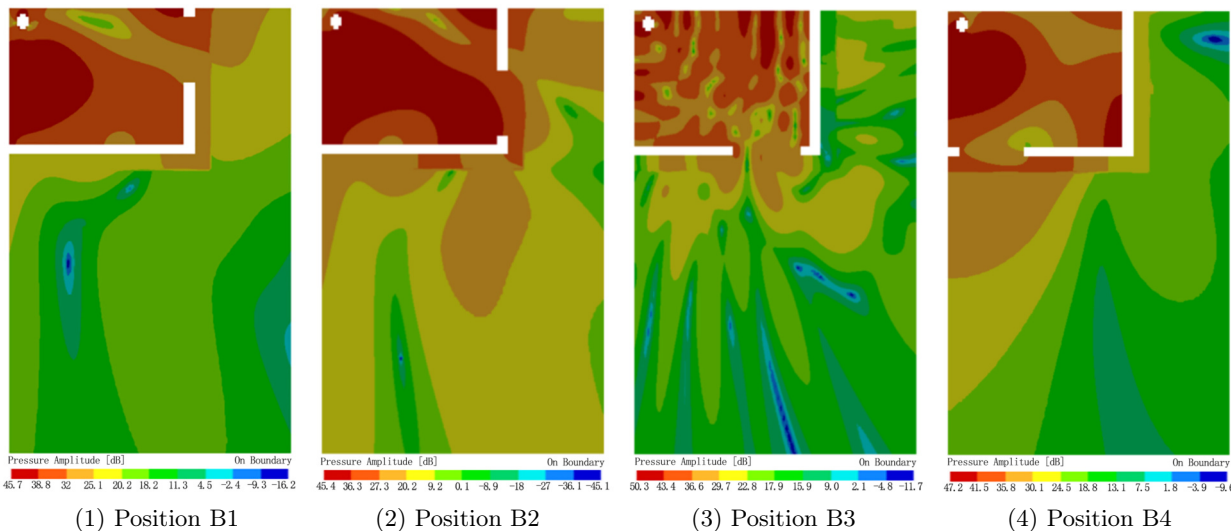
Analysis of the simulation cloud diagram and data shows that the pipe drainage noise has prominent high-frequency characteristics, and the sound pressure level is higher in the frequency range above 1000 Hz. The maximum noise level outside the pipe is distributed near the pipe, with the noise level gradually decreasing with increasing distance from the pipe. Analysis of the distribution cloud diagram of the planar sound pressure level indicates that the sound pressure level is significantly greater than that in the surrounding area of the connecting line between the riser and the door, and the difference between the middle- and high-frequency ranges can reach more than 10 dB.

The noise values of the monitoring points in the bedroom space for the B1, B2, B3, and B4 working conditions are 41.3 dB(A), 43.5 dB(A), 46.1 dB(A), and 43.2 dB(A), respectively, among which the noise value of the B3 working condition facing the bedroom space is greater than that of the other working conditions.

Table 5. Schematic representation of the structural modes of the partition wall.



a) 250 Hz



b) 500 Hz

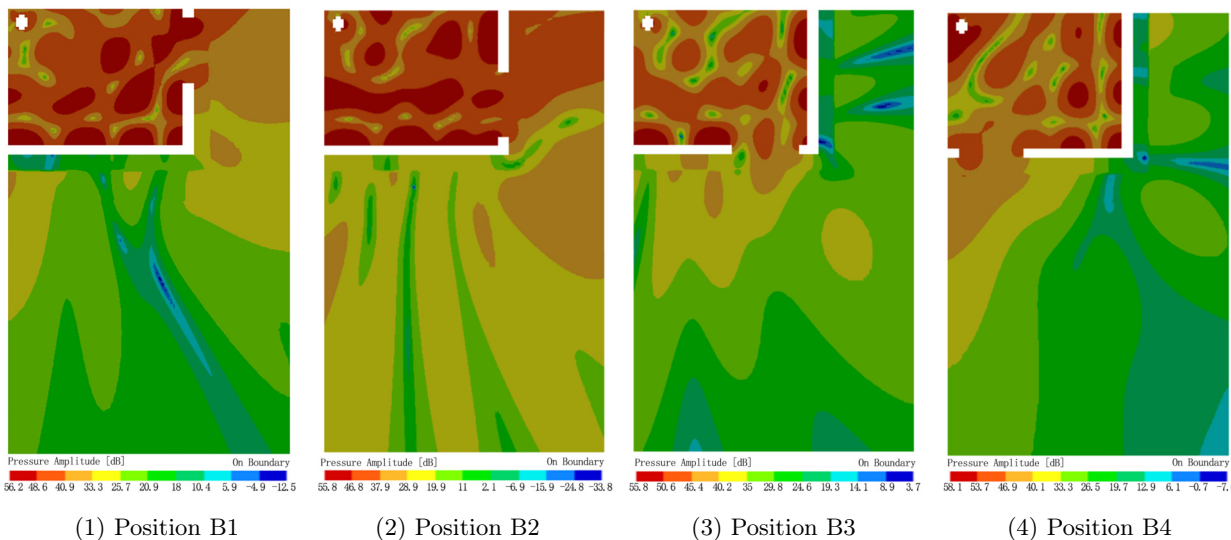
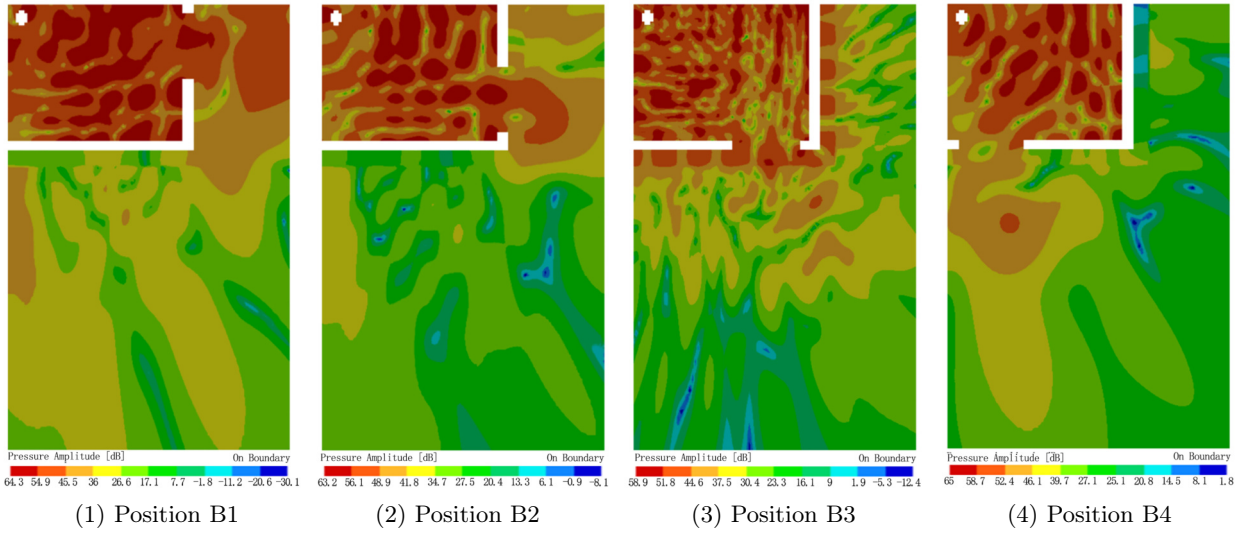
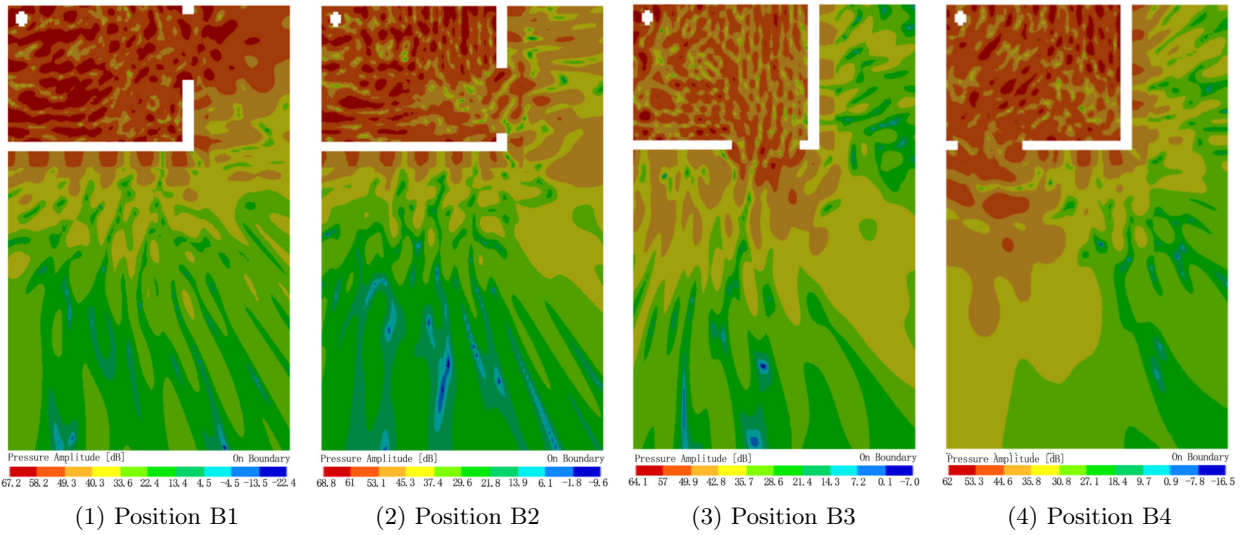


[Fig. 12ab.]

c) 1000 Hz



d) 2000 Hz



e) 4000 Hz

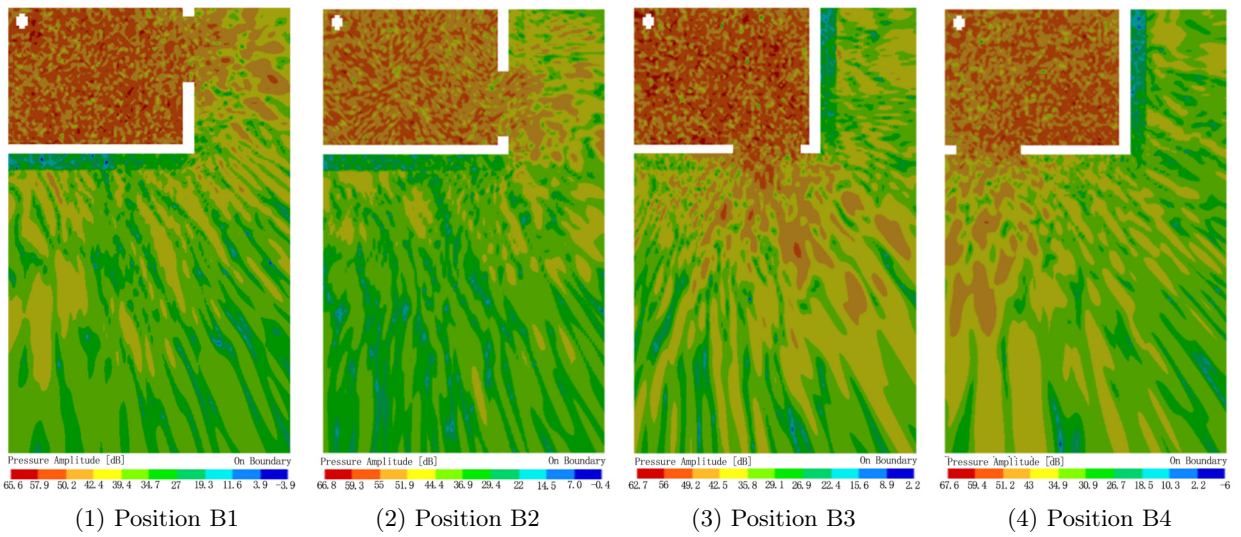


Fig. 12. Distribution of sound pressure levels in the external space at different door positions.

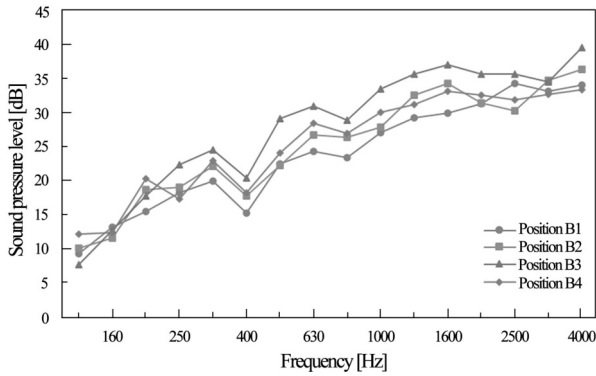


Fig. 13. Sound pressure levels at monitoring points.

When the door position corresponds to the B1 and B2 working conditions, the area with higher noise is mainly distributed at the entrance of the bedroom suite, and the impact on the noise in the bedroom space

is relatively small; under the B3 and B4 working conditions, as the relative angle between the door and the riser increases, the noise value of the indoor monitoring points increases.

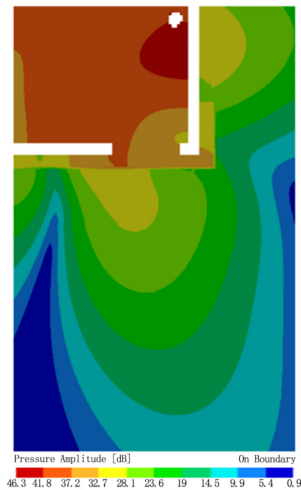
4.2.2. Influence of the riser position

To analyse the influence of the drainage riser position on the distribution of pipe drainage noise in the external space, the door position is configured for the Model 3, and the drainage noise distributions of the A3, B3, and C3 working conditions are calculated for different pipe positions.

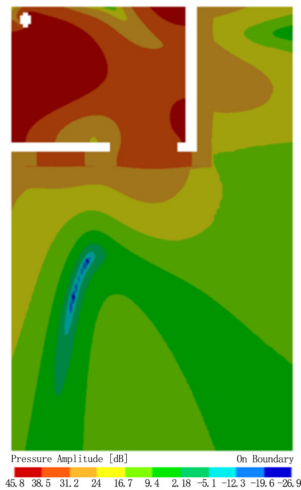
The external spatial sound field distribution of the riser at different positions is shown in Fig. 14, and the noise spectrum of the indoor monitoring points is shown in Fig. 15.

In a comparison of the calculations for different riser positions, when the riser positions are in the A3,

a) 250 Hz



(1) Riser position A3



(2) Riser position B3



(3) Riser position C3

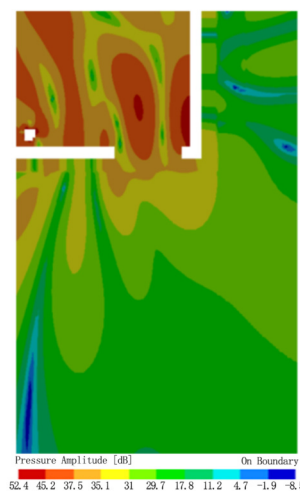
b) 500 Hz



(1) Riser position A3



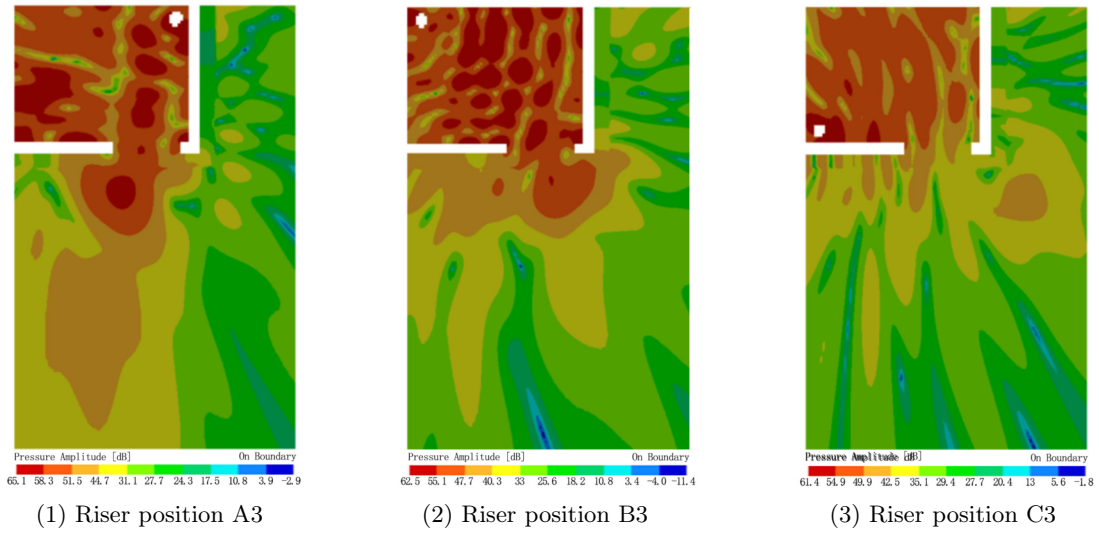
(2) Riser position B3



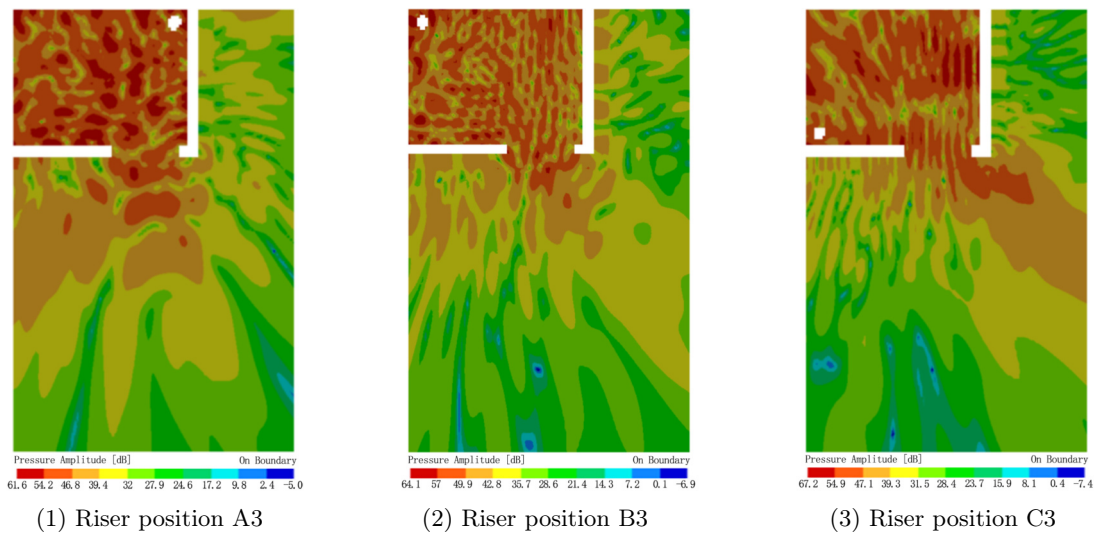
(3) Riser position C3

[Fig. 14ab.]

c) 1000 Hz



d) 2000 Hz



e) 4000 Hz

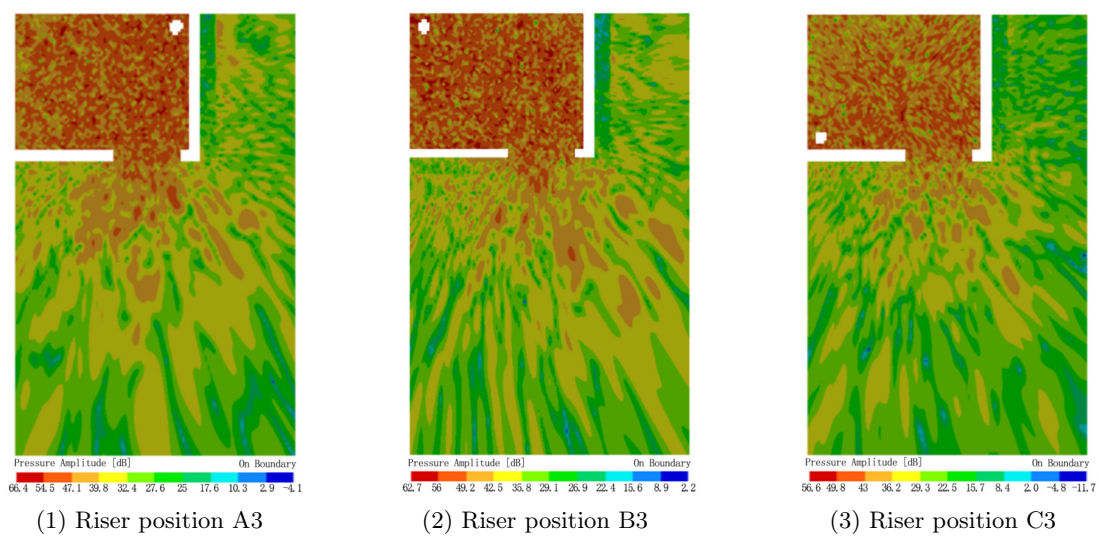


Fig. 14. Distribution of sound pressure levels in the external space at different riser positions.

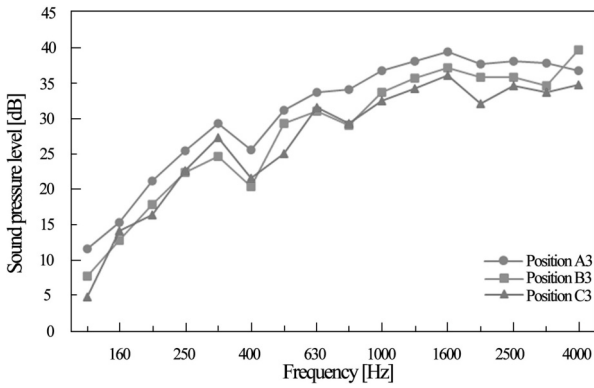


Fig. 15. Sound pressure levels at monitoring points.

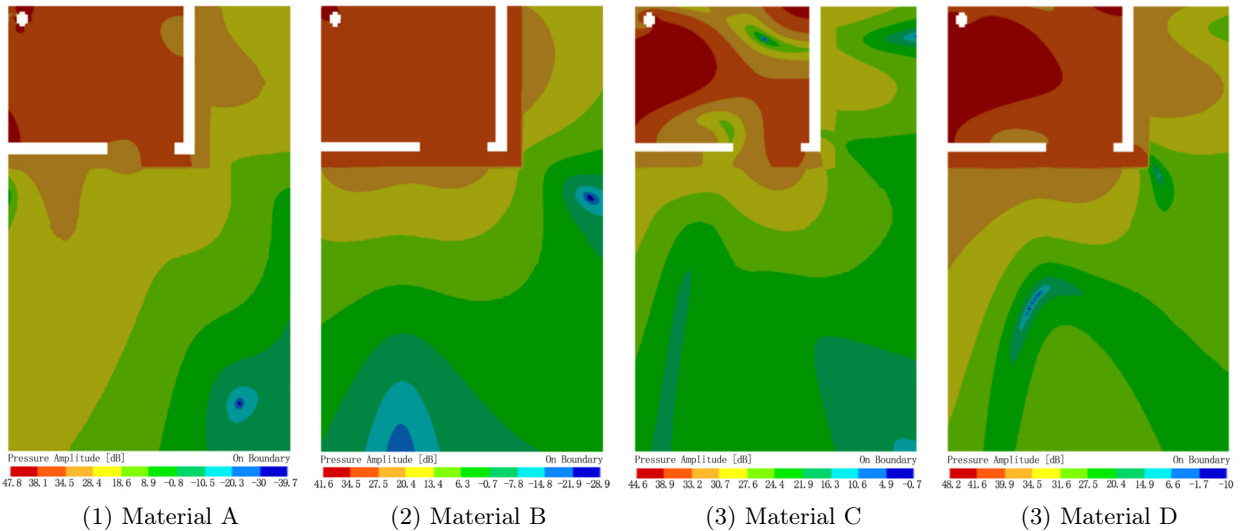
B3, and C3 working conditions, the pipe drainage noise values at the monitoring points in the bedroom are 48.2 dB(A), 46.1 dB(A), and 43.9 dB(A), respectively.

The A3 working condition has the highest noise impact because there is no direct shielding between the riser and the external space, so the drainage noise is directly transmitted to the outside.

4.2.3. Influence of the partition wall material

To analyse the influence of the bathroom partition wall material on the noise distribution in the external space, the partition wall material parameter is used as the dependent variable, and the position of the pipe and door is set to the B3 working condition. Common masonry materials are selected for the partition wall material, including ordinary fired brick masonry, ordinary concrete brick masonry, a lightweight aggregate concrete block wall, and a fly ash block wall, and the corresponding property setting parameters are shown in Table 6.

a) 250 Hz



b) 500 Hz

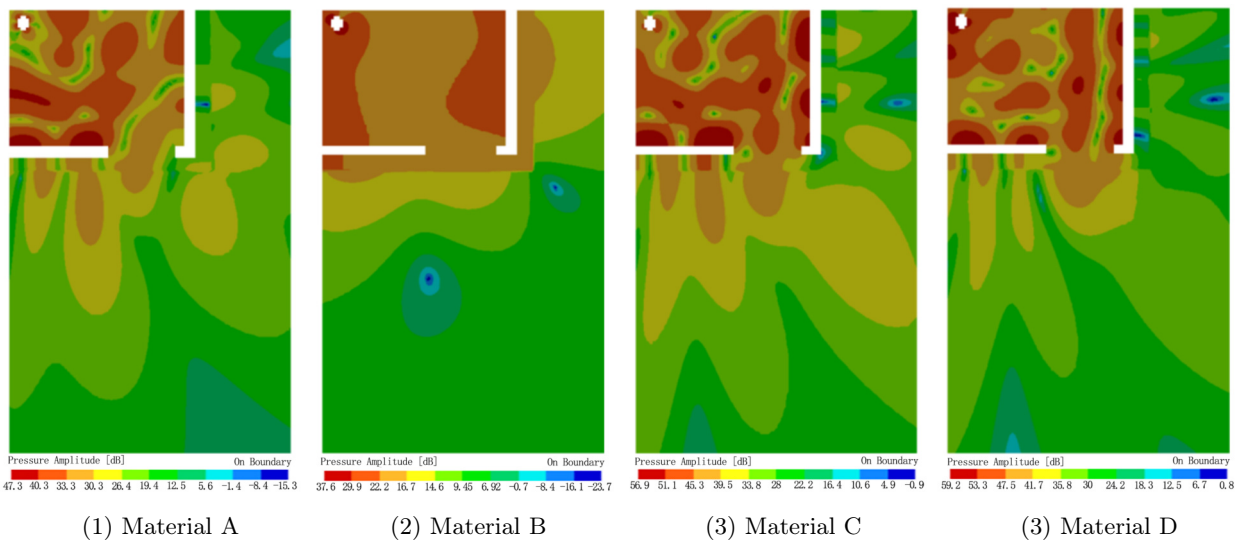
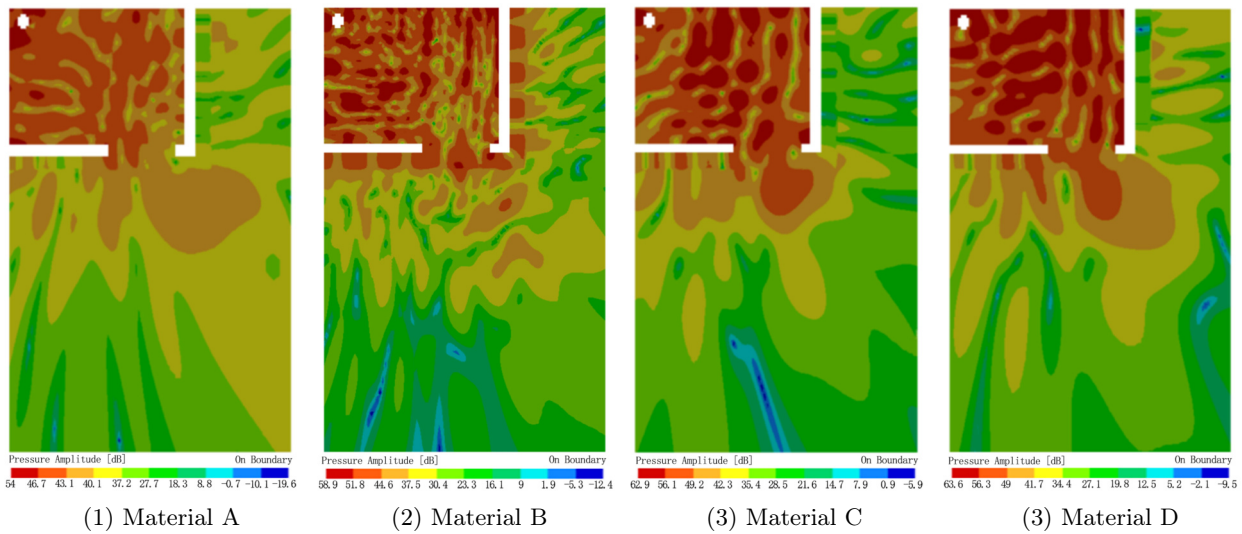
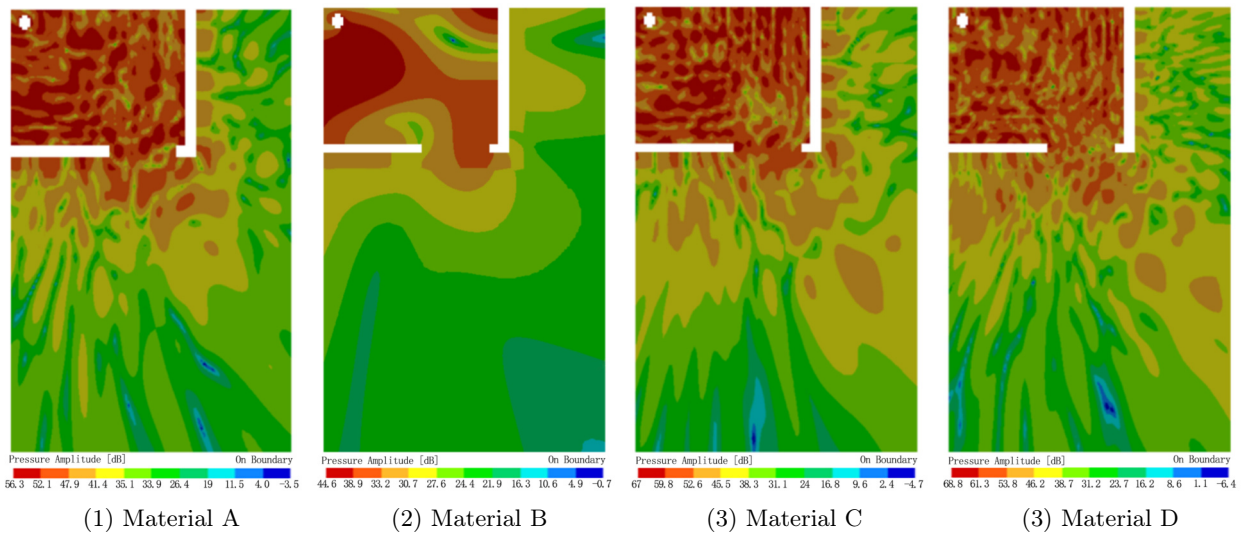


[Fig. 16ab.]

c) 1000 Hz



d) 2000 Hz



e) 4000 Hz

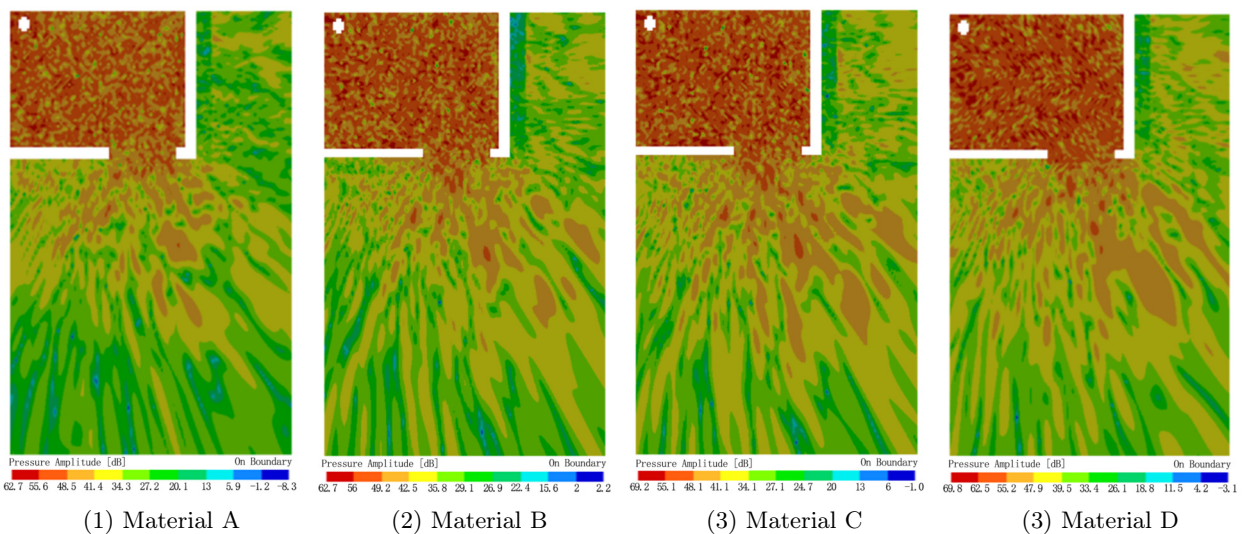


Fig. 16. Distribution of sound pressure levels in the external space for different partition materials.

Table 6. Materials for bathroom partitions.

Materials	Young's modulus [N/m ²]	Poisson's ratio	Density [kg/m ³]
Ordinary fired brick	4.4×10^9	0.15	1800
Ordinary concrete bricks	4.4×10^9	0.2	2000
Lightweight aggregate concrete block	3.4×10^9	0.2	1000
Fly ash block	2.83×10^9	0.2	1400

The sound field distribution in the external space with different partition wall materials. The results are shown in Fig. 16. The four materials in the diagram are represented by materials A, B, C, and D. The noise spectrum at the indoor monitoring point is shown in Fig. 17.

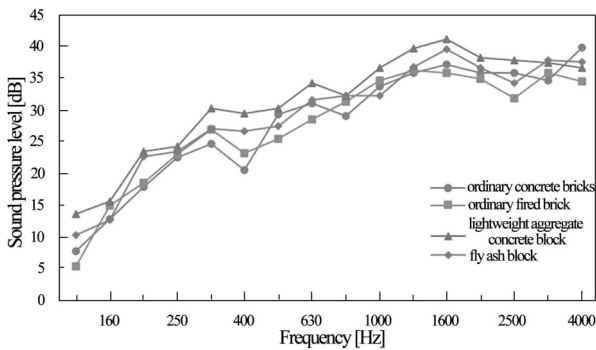


Fig. 17. Sound pressure levels at monitoring points.

A comparison of the noise data from the monitoring points in the bedroom shows that the noise gradually increases with increasing frequency, showing an increasing trend, with a few frequencies, such as 400 Hz, 800 Hz, and 2500 Hz, showing a slight decrease in the noise. The noise values of the monitoring points in the bedroom space under the four working conditions of ordinary concrete bricks, ordinary fired bricks, lightweight aggregate concrete blocks, and fly ash blocks are 46.1 dB(A), 44.6 dB(A), 48.1 dB(A) and 48.6 dB(A), respectively. When wall materials with higher masses, densities, and Young's moduli, such as ordinary concrete bricks and ordinary fired bricks, are used, the external space noise is slightly lower than that under working conditions with lightweight concrete and fly ash blocks. However, the difference between the noise values simulated under the four working conditions is not prominent.

5. Test of drainage noise

To verify the accuracy of the simulation results, the B3 working condition with the most simulated cases in Sec. 4 was chosen for the drainage noise field test to compare the results of the simulation and the test of drainage noise.

5.1. Test programme

The plan layout of the spaces within the test suite is shown in Fig. 18a. The partition wall between

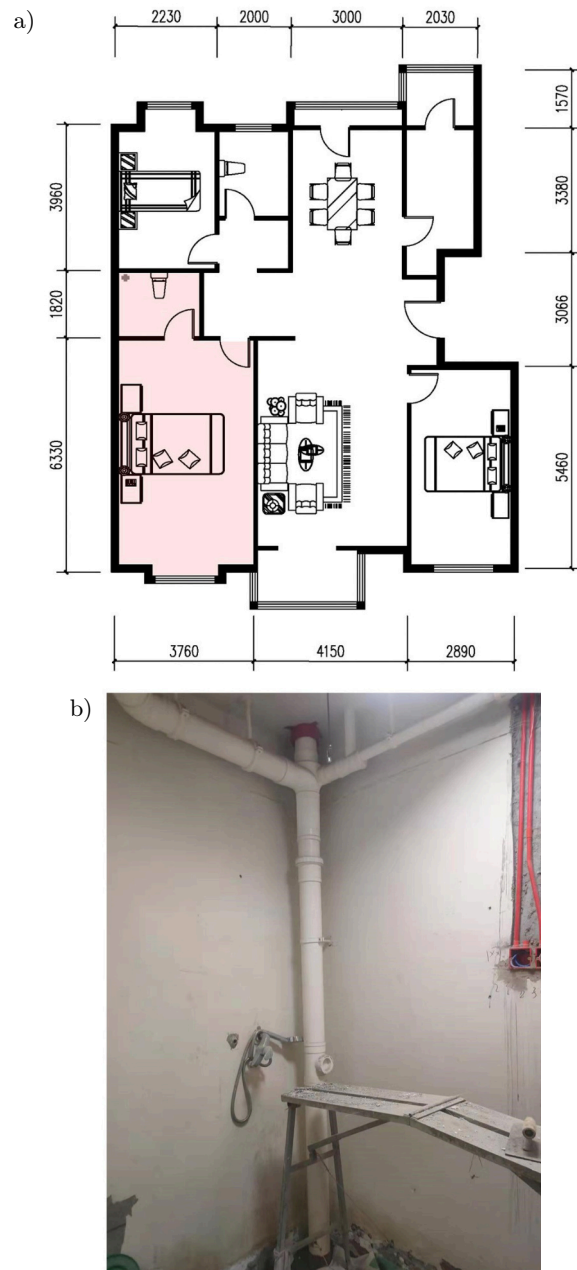


Fig. 18. Test condition master bedroom suite: a) plan layout of test condition; b) master bathroom riser.

the bathroom and the adjacent space is a 100 mm lightweight block wall. The sanitary ware is a toilet. A common UPVC single-riser drainage system with different floor drainage methods is used in the master bathroom, as shown in Fig. 18b. The riser in the master bathroom is located at the intersection of the second bedroom partition wall and the splitting wall, with the door opening towards the master bedroom. The layout is the same as that of the B3 working condition.

The field test consists of the indoor background noise and drainage noise. The background noise was measured with the doors and windows closed. During pipe drainage in the master bathroom, the noise in the adjacent space was measured under the most unfavourable conditions, that is, with the door open.

The test period was from 2 p.m.–4 p.m., and the instrument was a BK2260 precision noise analyser with a range of 0.8 dB–80 dB. The sound pressure level was measured at $1/3$ octave centre frequencies in the range of 10 Hz–20 kHz. The sound pressure level at the centre of the room is used to represent the noise level of the whole space according to the relevant specifications for sound pressure level testing, with the height of the measurement point being 1.2 m above the indoor floor.

5.2. Comparison of simulation and test results

A comparison of the simulated and tested sound pressure levels for the B3 working condition is shown in Fig. 19. When the doors and windows are closed, the background noise level during the day is 33.7 dB(A), as shown in Fig. 20. Analysis of the data shows that

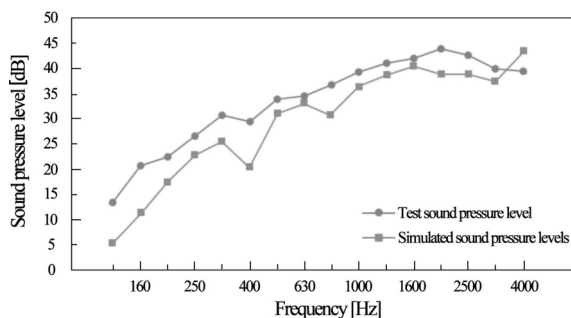


Fig. 19. Comparison of the sound pressure levels of simulations and tests.

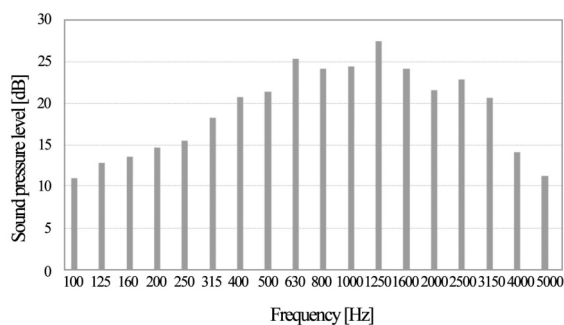


Fig. 20. Indoor daytime background noise.

the tested sound pressure level for drainage noise was 48.5 dB(A), which is 2.4 dB different from the simulated sound pressure level of 46.1 dB(A) for the B3 working conditions in Subsecs. 4.2.1 and 4.2.2, mainly due to the influence of background noise at the test site. Analysis of the sound pressure level frequency curves clearly shows that in the range of 125 Hz–3150 Hz, the test sound pressure level is slightly greater than the simulated sound pressure level, and in the range of 3150 Hz–4000 Hz, the simulated sound pressure level is slightly greater than the test sound pressure level, but the overall trend of the simulated and test sound pressure level frequency curves is similar. At the same time, both the simulated and tested sound pressure levels exhibit high-frequency characteristics, with the maximum noise occurring at approximately 1600 Hz–2000 Hz. A comparison of the conclusions shows that the results obtained by the numerical calculation method are consistent with the test results.

6. Conclusions

This paper analyses the causes and factors influencing bathroom drainage noise and uses the finite element numerical simulation technology with the help of the Fluent software and the LMS Virtual Lab to present a method to simulate the indoor drainage noise distribution using a joint simulation of the flow and sound fields. A three-dimensional model of the drainage noise computational domain, pipe wall, and partition wall was established to simulate the distribution of pipe drainage noise in the space under different working conditions, such as different door opening positions, riser arrangement positions, and partition wall materials. The conclusions are as follows:

- 1) The noise generated by drainage pipes increases with increasing frequency and has prominent high-frequency characteristics. Larger sound pressure levels often appear between high frequencies of 1600 Hz–2000 Hz.
- 2) The noise outside the pipe decreases gradually with an increasing distance from the pipe. The distribution of noise in the bedroom plane exhibits notable directionality due to the shielding and obstruction effect of the enclosure components. The sound pressure level near the connection line between the drainage riser and the door is greater than that of the surrounding area, and the difference increases with increasing frequency.
- 3) Among the four working conditions of the bathroom door position, the noise simulation value is 46.1 dB(A) when the bathroom door is arranged facing the used space, which is significantly greater than that under other working conditions. When the drainage riser is set towards the door, the simulated noise can reach 48.2 dB(A), which

is slightly greater than that under other working conditions. When the bathroom partition wall is made of four common materials – ordinary concrete bricks, ordinary fired bricks, lightweight aggregate concrete blocks, and fly ash blocks – the simulated noise at the bedroom monitoring point ranges from 44.6 dB(A) to 48.1 dB(A), and ordinary fired bricks have better sound insulation performance. Therefore, to reduce the interference of drainage noise from residential bathrooms, the position of bathroom doors, the position of pipes, and the construction of partition walls should be reasonably considered when designing building plans.

However, due to the limitations of the current level of the numerical simulation technology and the capabilities of the finite element simulation software, the three-dimensional model used in this paper has been simplified, and more ideal parameter settings have been adopted. However, it is hoped that the actual research and related conclusions in this paper can provide a reference for further research in the future.

Acknowledgments

This research did not receive any specific grant from funding agencies in the public, commercial, or non-profit sectors. The authors would like to sincerely thank the anonymous reviewers for their constructive suggestions, which have substantially improved the quality of this study.

References

- CAO Y., KE H., LIN Y., ZENG M., WANG Q. (2017), Investigation on the flow noise propagation mechanism in pipes of shell-and-tube heat exchangers based on synergy principle of flow and sound fields, *Applied Thermal Engineering*, **122**: 339–349, doi: [10.1016/j.applthermaleng.2017.04.057](https://doi.org/10.1016/j.applthermaleng.2017.04.057).
- CURLE N. (1955), The influence of solid boundaries upon aerodynamic sound, *Proceedings of the Royal Society of London, Series A. Mathematical and Physical Sciences*, **231**(1187): 505–514, doi: [10.1098/rspa.1955.0191](https://doi.org/10.1098/rspa.1955.0191).
- FFOWCS WILLIAMS J.E., HAWKINGS D.L. (1969), Sound generation by turbulence and surfaces in arbitrary motion, *Philosophical Transactions of the Royal Society of London, Series A, Mathematical and Physical Sciences*, **264**(1151): 321–342, doi: [10.1098/rsta.1969.0031](https://doi.org/10.1098/rsta.1969.0031).
- FUCHS H.V. (1983), Generation and control of noise in water supply installations: Part 1: Fundamental aspects, *Applied Acoustics*, **16**(5): 325–346, doi: [10.1016/0003-682x\(83\)90025-7](https://doi.org/10.1016/0003-682x(83)90025-7).
- FUCHS H.V. (1993a), Generation and control of noise in water supply installations. Part 2: Sound source mechanisms, *Applied Acoustics*, **38**(1): 59–85, doi: [10.1016/0003-682x\(93\)90041-4](https://doi.org/10.1016/0003-682x(93)90041-4).
- FUCHS H.V. (1993b), Generation and control of noise in water supply installations. Part 3: Rating and abating procedures, *Applied Acoustics*, **39**(3): 165–190, doi: [10.1016/0003-682x\(93\)90002-N](https://doi.org/10.1016/0003-682x(93)90002-N).
- HAN T. *et al.* (2020), Flow-induced noise analysis for natural gas manifolds using LES and FW-H hybrid method, *Applied Acoustics*, **159**: 107101, doi: [10.1016/j.apacoust.2019.107101](https://doi.org/10.1016/j.apacoust.2019.107101).
- JEON J.Y., JO H.I., KIM S.M., YANG H.S. (2019), Subjective and objective evaluation of water-supply and drainage noises in apartment buildings by using a head-mounted display, *Applied Acoustics*, **148**: 289–299, doi: [10.1016/j.apacoust.2018.12.037](https://doi.org/10.1016/j.apacoust.2018.12.037).
- JEONG A., KIM K., SHIN H., YANG K. (2017), Characteristics of reducing the water-drainage noise of toilet-bowl according to the composition of water drainage piping materials of the bathrooms of apartment housing [in Korean], *Transactions of the Korean Society for Noise and Vibration Engineering*, **27**(1): 114–120, doi: [10.5050/ksnve.2017.27.1.114](https://doi.org/10.5050/ksnve.2017.27.1.114).
- JIANG X., WU B. (2019), Design and exploration of drainage system based on pressure pipe in buildings, [in:] *IOP Conference Series: Earth and Environmental Science*, IOP Publishing, **300**(2): 022016, doi: [10.1088/1755-1315/300/2/022016](https://doi.org/10.1088/1755-1315/300/2/022016).
- JUNG H.Y., SUNG S.H., JUNG H.J. (2012), Drainage noise reduction system using a vacuum double pipe elbow, [in:] *Proceedings of the Korean Society for Noise and Vibration Engineering Conference*, pp. 817–818.
- LAU S.K., POWELL E.A. (2018), Effects of absorption placement on sound field of a rectangular room: A statistical approach, *Journal of Low Frequency Noise, Vibration and Active Control*, **37**(2): 394–406, doi: [10.1177/1461348418780027](https://doi.org/10.1177/1461348418780027).
- LIANG Z., ZHOU G., ZHANG Y., LI Z., LIN S. (2006), Vibration analysis and sound field characteristics of a tubular ultrasonic radiator, *Ultrasonics*, **45**(1–4): 146–151, doi: [10.1016/j.ultras.2006.07.022](https://doi.org/10.1016/j.ultras.2006.07.022).
- LIGHTHILL M.J. (1952), On sound generated aerodynamically. I. General theory, *Proceedings of the Royal Society of London, Series A. Mathematical and Physical Sciences*, **211**(1107): 564–587, doi: [10.1098/rspa.1952.0060](https://doi.org/10.1098/rspa.1952.0060).
- LIU E., YAN S., PENG S., HUANG L., JIANG Y. (2016), Noise silencing technology for manifold flow noise based on ANSYS fluent, *Journal of Natural Gas Science and Engineering*, **29**: 322–328, doi: [10.1016/j.jngse.2016.01.021](https://doi.org/10.1016/j.jngse.2016.01.021).
- MAO Q., PIETRZKO S. (2013), *Control of noise and structural vibration*, Springer, London, pp. 3–4, doi: [10.1007/978-1-4471-5091-6](https://doi.org/10.1007/978-1-4471-5091-6).
- MARBURG S., NOLTE B. [Eds.] (2008), *Computational Acoustics of Noise Propagation in Fluids: Finite and Boundary Element Methods*, Springer, Berlin, doi: [10.1007/978-3-540-77448-8](https://doi.org/10.1007/978-3-540-77448-8).

18. Ministry of Housing and Urban-Rural Development of China (2019), *Standard for design of building water supply and drainage (GB 50015-2019)* [in Chinese], China Planning Press, Beijing, China.
19. MORI M., MASUMOTO T., ISHIHARA K. (2017), Study on acoustic, vibration and flow induced noise characteristics of T-shaped pipe with a square cross-section, *Applied Acoustics*, **120**: 137–147, doi: [10.1016/j.apacoust.2017.01.022](https://doi.org/10.1016/j.apacoust.2017.01.022).
20. NORTON M.P., BULL M.K. (1984), Mechanisms of the generation of external acoustic radiation from pipes due to internal flow disturbances, *Journal of Sound and Vibration*, **94**(1): 105–146, doi: [10.1016/s0022-460x\(84\)80008-5](https://doi.org/10.1016/s0022-460x(84)80008-5).
21. NORTON M.P., KARZUB D.G. (2003a), Pipe flow noise and vibration: a case study, [in:] *Fundamentals of Noise and Vibration Analysis for Engineers*, Cambridge University Press, Cambridge, pp. 441–487, doi: [10.1017/cbo9781139163927.009](https://doi.org/10.1017/cbo9781139163927.009).
22. NORTON M.P., KARZUB D.G. (2003b), Mechanical vibrations: a review of some fundamentals, [in:] *Fundamentals of Noise and Vibration Analysis for Engineers*, Cambridge University Press, Cambridge, pp. 1–127, doi: [10.1017/cbo9781139163927.003](https://doi.org/10.1017/cbo9781139163927.003).
23. PARK S.H., LEE P.J., JEONG J.H. (2018), Effects of noise sensitivity on psychophysiological responses to building noise, *Building and Environment*, **136**: 302–311, doi: [10.1016/j.buildenv.2018.03.061](https://doi.org/10.1016/j.buildenv.2018.03.061).
24. PUJOL S. et al. (2014), Indoor noise exposure at home: a field study in the family of urban schoolchildren, *Indoor air*, **24**(5): 511–520, doi: [10.1111/ina.12094](https://doi.org/10.1111/ina.12094).
25. RYU J., SONG H. (2019), Comparison between single-number quantities for rating noises from sanitary installations in residential buildings by objective and subjective methods, *Building and Environment*, **164**: 106378, doi: [10.1016/j.buildenv.2019.106378](https://doi.org/10.1016/j.buildenv.2019.106378).
26. SUN L., ZHE C., GUO C., CHENG S., HE S., GAO M. (2021), Numerical simulation regarding flow-induced noise in variable cross-section pipes based on large eddy simulations and Ffowcs Williams–Hawkings methods, *AIP Advances*, **11**(6): 065118, doi: [10.1063/5.0052148](https://doi.org/10.1063/5.0052148).
27. Standardization Administration of the P.R.C. (2008), *Functions and dimensions series of bathrooms in housing (GB 11977-2008)* [in Chinese], China Quality and Standards Publishing and Media Co., Ltd., China.
28. VILLOT M. (2000), Characterization of building equipment, *Applied Acoustics*, **61**(3): 273–283, doi: [10.1016/S0003-682X\(00\)00034-7](https://doi.org/10.1016/S0003-682X(00)00034-7).
29. XU N., ZHANG C., MA L. (2014), Residential building sound pollution and control measures, *Advanced Materials Research*, **945**: 711–716, doi: [10.4028/www.scientific.net/amr.945-949.711](https://doi.org/10.4028/www.scientific.net/amr.945-949.711).
30. YANG H.S., CHO H.M., KIM M.J. (2016), Field measurements of water supply and drainage noise in the bathrooms of Korea’s multi-residential buildings, *Applied Acoustics*, **6**(11): 372, doi: [10.3390/app6110372](https://doi.org/10.3390/app6110372).
31. YEON J.O., KIM K.W., YANG K.S., LEE B.K. (2014), Evaluation of noise characteristics of drainage and water supply systems in apartment bathrooms, *Advanced Materials Research*, **1025**: 987–990, doi: [10.4028/www.scientific.net/amr.1025-1026.987](https://doi.org/10.4028/www.scientific.net/amr.1025-1026.987).
32. ZHANG N., XIE H., XING W., WU B. (2016), Computation of vortical flow and flow induced noise by large eddy simulation with FW-H acoustic analogy and Powell vortex sound theory, *Journal of Hydrodynamics*, **28**(2): 255–266, doi: [10.1016/s1001-6058\(16\)60627-3](https://doi.org/10.1016/s1001-6058(16)60627-3).